# Impact of the substrate composition on enhanced biological phosphorus removal during formation of aerobic granular sludge

# Impact of the substrate composition on enhanced biological phosphorus removal during formation of aerobic granular sludge

**Authors**

Lennert Dockx[1], lennert.dockx@uantwerpen.be

Michel Caluwé[1], michel.caluwe@uantwerpen.be

Flinn De Vleeschauwer[1], flinn.devleeschauwer@uantwerpen.be

Thomas Dobbeleers[1], thomas.dobbeleers@uantwerpen.be

Jan Dries[1], jan.dries2@uantwerpen.be (Corresponding author)

**Affiliations**

[1]BioWAVE, Biochemical Wastewater Valorization and Engineering, Faculty of Applied Engineering, University of Antwerp, Groenenborgerlaan 171, 2020 Antwerpen, Belgium

**Abstract**

Performance of enhanced biological phosphorus removal (EBPR) is often investigated with simple synthetic wastewater containing volatile fatty acids (VFAs). In this study, various (fermentable) substrates, individually and in mixtures, were examined during the application of a granulation strategy. In addition, the microbial community and $N_2O$ formation were monitored. Sludge densification was observed in all systems. Stable EBPR, associated with the presence of *Accumulibacter* and an anaerobic phosphorus-release up to 21.9 $mgPO_4^{3-}$-P.$gVSS^{-1}$, was only obtained when VFAs were present as sole substrate or in mixture. Systems fed with VFAs were strongly related to the formation of $N_2O$ (maximum of 6.25% relative to the total available nitrogen). A moderate anaerobic dissolved organic carbon (DOC) uptake was observed when amino acids (64.27 ± 3.08%) and glucose (75.39 ± 5.79%) as sole carbon source were applied. The substrate/species-specific enrichment of *Burkholderiaceae* and *Saccharimonadaceae* respectively, resulted in unstable EBPR in those systems.

**Keywords**

aerobic granular sludge; denitrifying phosphate accumulating organisms; $N_2O$; synthetic wastewater; 16S rRNA gene amplicon sequencing

## 1. Introduction

The aerobic granular sludge (AGS) technology offers a low-footprint (up to 75% reduction) and cost-effective (25-55% reduction in energy demand) wastewater treatment process with high biomass concentrations (8-10 $g.L^{-1}$) and improved sludge/water separation due to fast settling properties (Pronk et al., 2015). AGS relies on a specific operation that promotes the growth of so-called 'slow-growing' microorganisms which first store carbon as storage polymers (e.g. polyhydroxyalkanoates (PHA)) during the (anaerobic) feast phase and subsequently consume the stored carbon for growth during the (aerobic) famine phase (de Kreuk & van Loosdrecht, 2004). These organisms produce a significant amount of structural extracellular polymer substances (EPS) to form a hydrogel matrix (Felz et al., 2019). In many laboratory studies on AGS, researchers used easily degradable and diffusible substrates, more specifically volatile fatty acids (VFAs) such as acetate and/or propionate, as sole carbon source in synthetic feeding media. Most of these studies report *Candidatus Accumulibacter phosphatis* as well as *Candidatus Competibacter phosphatis* as most abundant organisms (Henriet et al., 2016; Weissbrodt et al., 2014). A minority of studies on AGS were performed with wastewater containing polymeric substances (Adler & Holliger, 2020; Layer et al., 2019). Complex substrates will leak in the aerobic phase as they cannot be readily taken up anaerobically by bacteria before undergoing hydrolysis (de Kreuk et al., 2010). The negative impact on granule formation linked to chemical oxygen demand (COD) that is not stored during the anaerobic phase and leaks into the aerobic phase is extensively reported (Wagner et al., 2015b; Wang et al., 2018).

Enhanced biological phosphorus removal (EBPR) is an alternative for conventional removal of phosphorus (P) by coagulation/flocculation using chemical reagents such as ferric chloride ($FeCl_3$). Polyphosphate-accumulating organisms (PAOs) are bacteria able to perform EBPR by their PHA related storage metabolism (Nielsen et al., 2012). The current biochemical EBPR model is based on the most widely known PAO, namely, *Accumulibacter* (Oehmen et al., 2010). However, the contribution of *Accumulibacter* towards EBPR in full-scale plants is still under debate (Nielsen et al., 2019). Research shows that the PAO diversity in conventional EBPR treatment plants is much wider and certainly not limited to *Accumulibacter* (Stokholm-Bjerregaard et al., 2017). Bacteria from the actinobacterial genus were the most abundant PAOs in 18 non-granular full-scale Danish EBPR plants. The genera *Tetrasphaera* and *Dechloromonas* were identified, while *Accumulibacter* species were much less abundant. Recent work reported the presence of other genera in AGS reactors treating more complex wastewater (Dobbeleers et al., 2020; Layer et al., 2019; Stes et al., 2018). In contrast to *Accumulibacter* that only uses VFAs as primary substrate (Marques et al., 2017), *Tetrasphaera* seems to have a more versatile physiology which results in the assimilation of different organic substances (e.g. amino acids and glucose) (Nielsen et al., 2012). EBPR is based on the ability of PAOs to take up P and accumulate it intracellularly in the form of polyphosphate (poly-P) when exposed to alternating anaerobic/aerobic and/or anaerobic/anoxic conditions. The latter case is very interesting in terms of biological nutrient removal (BNR) since nitrogen (N) and P can be simultaneously removed (i.e. d-EBPR) by denitrifying PAOs (d-PAOs), under anoxic conditions (cfr. simultaneous nitrification/denitrification (SND)) (Carvalho et al., 2007).

In detail, d-PAOs simultaneously remove P and nitrate in the anoxic zones, which typically occur in the core as a result of the oxygen-gradient within the granule (van den Berg et al., 2020). In this perspective, some *Accumulibacter* clades were already identified as important d-PAO (Rubio-Rincón et al., 2017). Of particular concern in BNR processes is the related emission of nitrous oxide ($N_2O$), with a 300 times higher greenhouse potential than $CO_2$ (EPA, 2017). $N_2O$ can be formed during nitrification and as the end product of an incomplete denitrification (Jahn et al., 2019; Kampschreur et al., 2009). A main factor stimulating formation of $N_2O$ is the PHA related denitrification (d-PAO) metabolism which is described as a first-order process. The slow degradation process of PHA influences the activity of $N_2O$ reductase (nosZ), leading to an accumulation of $N_2O$ during electron donor limiting conditions. Furthermore, $N_2O$ formation can be attributed to the lack of the nosZ gene in the genome of some organisms (Morales et al., 2010; Vieira et al., 2018). It was observed that the potential for $N_2O$ production was significantly higher than the potential for its reduction in systems enriched by *Accumulibacter*.

Industrial (complex polymeric) wastewater of food- and meat processing companies contains a mixture of organic substances, like proteins and carbohydrates (Dobbeleers et al., 2020; Stes et al., 2018). Knowledge acquired on AGS treating simple wastewater cannot be easily transferred to AGS treating more complex wastewater (Layer et al., 2019). This study examines carbon substrates, other than the widely applied VFAs, such as amino acids and glucose which are fermentable end products of the hydrolysis of proteins and carbohydrates. This study aims to investigate the effect

of these individual substrates on: (1) the process performance (P and N cycling) during AGS formation, (2) the microbial community, and (3) $N_2O$ formation.

## 2. Material and methods

### 2.1. Influent composition

Five reactors were fed with synthetic wastewater (1500 mg COD.$L^{-1}$). The composition (% of COD) during the entire study was kept constant. This study was performed in two stages (stage I (142 days) and stage II (62 days)). In both stages of the study a reference reactor, fed with a mixture of acetate (50%) and propionate (50%), was included (SBR A and D). During stage I (SBR A, B and C) single-type carbon substrates were applied. The influent of SBR B consisted of a mixture of amino acids (leucine (33%), aspartic acid (33%) and glutamic acid (33%)) while SBR C was fed with glucose (100%) as carbon substrate. N and P dosage was performed using respectively $NH_4Cl$ and $K_2HPO_4$. As amino acids already contribute to the N content, an adapted $NH_4Cl$ dosage was performed to achieve a similar COD/N ratio in all reactors. The influent composition during stage I resulted in a COD/N ratio of 11 and a COD/P ratio of 50. In Stage II (SBR E) a mixture of substrates (acetate (16.5%), propionate (16.5%, aspartic acid (16.5%), glutamic acid (16.5%) and glucose (33%)) was used. In stage II, the COD/N ratio and COD/P ratio were 20 and 50 respectively. Additional nutrients were added in the following concentrations: 24mg $Mg^{2+}.L^{-1}$ ($MgSO_4.7H_2O$), 56mg $K^+.L^{-1}$ (KCl) and 1mL.$L^{-1}$ Trace Elements solution (Vishniac & Santer, 1957).

### 2.2. Reactor set-up and Operating Conditions

All reactor systems in this study were identical double-walled fully automated lab-scale SBRs (H/D = 1.66) with a working volume of 12L. A MX07R-20 refrigerated circulating bath (VWR International, Belgium) was used to control the temperature

within the systems. The temperature varied between 18°C and 22°C. Each reactor was equipped with an Iwaki® electromagnetic metering feeding pump (ES-B16VC-3) (IWAKI, Japan) and a discharge valve (Eriks RX10.X33.S00) (ERIKS nv, Belgium). To supply the reactor with oxygen a Super Fish Koi Flow 60 (AQUADISTRI, China) was connected to an air disc diffuser (diameter of 13cm) (AQUADISTRI, China). A Heidolph® mixer (RZR 2041) (Heidolph Instruments GmbH & Co.KG, Germany) and propeller (R 1345) (IKA®-Werke GmbH & Co. KG, Germany) were used to keep the sludge in suspension. Hardware actions associated with the SBR operation were automatically controlled with a PLC (Siemens, Germany) which could be manipulated by a custom-build LabView™ supervision program (National Instruments, United States). Each reactor contained a luminescent dissolved oxygen (DO) sensor (Hach Lange®, United States), pH JUMO® Tecline sensor (JUMO GmbH & Co.KG, Germany) and conductivity JUMO® BlackLine sensor (JUMO GmbH & Co.KG, Germany). Data logging was performed with a Lange sc1000 (Hach Lange®, United States). The DO level during the aerobic step was controlled with an on/off aeration control, between 1.0 and 2.0 mg $O_2.L^{-1}$. The oxygen uptake rate (OUR) was calculated as previously reported (Dobbeleers et al., 2017).

All five reactors were inoculated with (flocculent) activated sludge from a local low-loaded BNR municipal wastewater treatment plant (Aquafin Antwerpen-Zuid), processing domestic wastewater. An anaerobic feast/aerobic famine regime was applied in all reactors to stimulate AGS formation. In stage I, the reactor cycle involved the following steps: non-aerated mixed phase (10min), anaerobic mixed influent pulse feeding (from the top) (16min), anaerobic reaction (74min), aerobic reaction (280min),

anoxic reaction (60min), sludge settling (30min), effluent (5min) and idle (5min). In stage II, the aerobic period was decreased (165min) resulting in a total cycle time of 6h instead of 8h. In both stages, an influent feed of 1.5L resulted in a volume exchange rate (VER) of 12.5%. By removing excess biomass from the reactor at the end of the anoxic reaction, the food to microorganism ratio (F/M) and SRT were controlled at 0.20 ± 0.02 kgCOD.(kgVSS.day)$^{-1}$ and 25-30 days respectively. The organic loading rate (OLR) was kept constant at 0.56 kgCOD.(m$^3$.d)$^{-1}$ (stage I) and 0.75 kgCOD.(m$^3$.d)$^{-1}$ (stage II).

### 2.3. Analyses

All samples were filtered using glass microfiber filters (particle retention 1.2 µM) from VWR International (Belgium). Chemical analyses, ammonium ($NH_4^+$-N), nitrite ($NO_2^-$-N), nitrate ($NO_3^-$-N), orthophosphate ($PO_4^{3-}$-P) and chemical oxygen demand (COD) were analysed with test kits from Hanna Instruments (Belgium) respectively HI93715-01, HI93707-01, HI93766-50, HI93706-01, HI93754A-25 and HI93754B-25. Dissolved organic carbon (DOC) was measured using a Sievers InnovOx Laboratory Total Organic Carbon Analyzer (General Electric Company, United States).

The evolution of biomass morphology (i.e. “degree of granulation”) was observed using the $SVI_5/SVI_{30}$ ratio (SVI respectively after 5 min ($SVI_5$) and 30 min ($SVI_{30}$) settling) and analysis of the size distribution (DV50) (Malvern Mastersizer 3000, Malvern Panalytical, United Kingdom) (Caluwe et al., 2017). The DV50 value is the 50$^{th}$ percentile of the cumulative distribution and is reported as a measure for the overall size distribution. It is the maximum particle diameter below which 50% of the sample volume exists. EPS extraction (using sodium carbonate) and analysis of gel-forming

capacity (using calcium chloride) of the extracted EPS were performed, according to Felz et al. (2019). Biomass concentrations, measured as mixed liquor (volatile) suspended solids (ML(V)SS) and sludge volume index (SVI) were determined according to Standard Methods (American Public Health Association (APHA), 2012).

### 2.4. *In-situ* cycle measurements

At regular time points, *in-situ* cycle measurements of all reactors were carried out to determine the anaerobic DOC uptake (%) and related P-release (mgP.gVSS$^{-1}$).

$$Anaerobic\ DOC\ uptake\ (\%) = \frac{DOC_{after\ feeding}\left(\frac{mg}{L}\right) - DOC_{end\ of\ anaerobic\ period}\left(\frac{mg}{L}\right)}{DOC_{after\ feeding}\left(\frac{mg}{L}\right) - DOC_{end\ of\ aerobic\ period}\left(\frac{mg}{L}\right)} * 100 \quad \text{[Equation 1]}$$

$$Anaerobic\ PO_4^{3-} - P\ release\ (mgP/gVSS) = \frac{\left(PO_{4\ end\ of\ anaerobic\ period}^{3-}\left(\frac{mg}{L}\right) * 12L\right) - \left(\left(PO_{4\ before\ feeding}^{3-}\left(\frac{mg}{L}\right) * 10.5L\right) + \left(PO_{4\ included\ in\ feeding}^{3-}\left(\frac{mg}{L}\right) * 1.5L\right)\right)}{MLVSS\left(\frac{mg}{L}\right) * 12L} \quad \text{[Equation 2]}$$

The degree of SND was estimated using the total amount of $NO_x$-N formed at the end of the aerobic step, divided by the amount of $NH_4^+$-N oxidized, with $t_0$ as start of the aeration and $t_e$ as end of the aeration. $NH_4^+$-N assimilation related to biomass growth was taken into account using the observed activated sludge yield ($\Delta x_v$) and a N-content of 0.1 gN.gVSS$^{-1}$ (Wagner et al., 2015a).

$$SND(\%) = 1 - \frac{[NO_x^-]_{t_0}^{t_e}}{[NH_4^+]_{t_e}^{t_0}} * 100 \quad \text{[Equation 3]}$$

### 2.5. $N_2O$ measurements and calculation

$N_2O$ profiles were monitored during *in-situ* cycle measurements. A Unisense® micro sensor (Aarhus, Denmark) with data logger was used to measure the $N_2O$ concentration in the liquid phase. A three-point calibration was done before each *in-*

*situ* cycle measurement test. The $N_2O$ emissions were calculated as described earlier by Dobbeleers et al. (2017).

### 2.6. *Ex-situ* batch experiments

The quantification of the specific nitrogen removal rates and NOB (nitrite oxidizing bacteria)/AOB (ammonia oxidizing bacteria) activity ratio was performed according to Dobbeleers et al. (2017).

To examine the influence of the individual carbon substrates on the EBPR activity, batch tests were performed at the end of each stage, for each SBR. The experiments involved the dosage of individual carbon substrates to sludge from the corresponding SBR and to sludge from reactors that did not receive these substrates during reactor operation. 300mL of sludge was taken out of the reactor at the end of the SBR cycle and washed (3 times) with a wash buffer (0.1M $NaHCO_3$ + 0.05M KCl). Individual carbon substrates were dosed using the same COD loading as applied in the SBRs. The MLVSS concentration, DOC uptake (%) and P-release ($mgP.gVSS^{-1}$) during the anaerobic period (90 min), were determined for each batch test.

### 2.7. Molecular quantification

#### 2.7.1. qPCR

At regular time points, three biological replicates (500µL) were taken. DNA extraction was carried out with NaTCA method including grinding step using pellet pestles (Z359971, Sigma-Aldrich, United States) (Caluwe et al., 2017). Concentrations of the extracted DNA were measured with a Qubit™ 3.0 Fluorometer (Thermo Fisher Scientific, United States). Absolute quantification of target organisms was done through SYBR Green quantitative polymerase chain reaction (qPCR) assays

(SSoAdvanced Universal SYBR Green® Supermix, Bio-Rad, United States) (Caluwe et al., 2017; Dobbeleers et al., 2017). qPCR was performed on a CFX96 Touch™ Real-Time PCR Detection System (Bio-Rad, United States). All qPCR assays contained three no-template control reactions. The amount of target cells per gVSS were calculated from the measured DNA and biomass concentrations according to Caluwe et al. (2017).

#### 2.7.2. 16S rRNA gene amplicon sequencing

qPCR results were confirmed by 16S rRNA gene amplicon sequencing on three biological replicates (500µL) (Dobbeleers et al., 2020). Amplicons targeting the V1-V3 region of the 16S rRNA gene were generated with barcoded primers (IDT) and Phusion High-Fidelity DNA Polymerase (Thermo Scientific, United States) (Kozich et al., 2013). PCR products were purified using the Agencourt AMPure XP PCR Purification Kit (Beckman Coulter, United States). After pooling, the resulting library was further purified by gel extraction using NucleoSpin Gel and PCR Clean-up (Macherey Nagel, United States). The enhanced purified library (4nM) was analysed at the Centre for Medical Genetics (Antwerp), where amplicon sequencing on a Illumina MiSeq system, using a MiSeq Reagent Kit v3 (Illumina, United States), was carried out. A similarity threshold of 97% was used. Taxonomy prediction of the OTU sequences were carried out with MiDAS 3.7 (Microbial Database for Activated Sludge) as reference database (Nierychlo et al., 2020). Further data analysis was done in R, using the ampvis2 package (Andersen et al., 2018) and the vegan 2.2.1 package (Oksanen et al., 2015).

## 3. Results and discussion

### 3.1. Reactor performance

The removal efficiency of total and soluble COD was higher than 93% in all systems. $PO_4^{3-}$-P removal efficiency, indicating the achievement of an EBPR process, varied

between the different reactor systems. Stable EBPR is defined as the situation when the effluent P concentration fulfils the local (Flemish) discharge limits (2.5 mg $P.L^{-1}$) and remains below 2.5 mg $P.L^{-1}$. During stage I, in SBR A (reference reactor fed with VFAs) an overall P-removal efficiency of 99.3 ± 0.9% was obtained. SBR B (fed with amino acids) showed a very variable P-removal of 80.6 ± 19.7%. In SBR B, the removal efficiencies ranged from 96% to less than 38%, confirming the results of Zengin et al. (2011) where an effective EBPR could not be maintained in amino acids fed systems. The deterioration of EBPR activity in systems fed with amino acids was associated with the limited availability of VFAs in the bulk solution resulting in an unstable presence of *Candidatus Accumulibacter* (Zengin et al., 2011). P-removal in SBR C (fed with glucose) was 74.9 ± 10.5%. A minimum of 65% P-removal (average of 73.9 ± 7.9%) in SBR C indicates the relative stable but insufficient P-removal during the entire study. During stage II, SBR D (reference reactor) achieved an overall $PO_4^{3-}$-P removal efficiency of 98.6 ± 1.0%. SBR E (fed with all substrates) obtained an overall efficiency of 98.7 ± 1.2%. This observation confirms the outcome of Adler & Holliger (2020) as they state that the presence of both fermentable substrates (cfr. amino acids and glucose) and VFAs (up to 33% of the OLR) did not negatively affect P-removal. Table 1 summarises the effluent $PO_4^{3-}$-P concentrations and P-removal efficiencies of all SBRs and indicates that only SBRs fed with VFAs in the influent fulfilled the local discharge limits (2.5 mg $PO_4^{3-}$-$P.L^{-1}$).

The $NH_4^+$-N removal efficiency was higher than 99% in all systems. Table 1 shows the overall total N-removal efficiency in each system. At the start of stage I, the degree of SND in the reactors was 16% and reached 21% and 44% in SBR A and SBR B

respectively at the end of the experiment. In SBR C, the degree of SND decreased and was about 5%. No $NO_2^-$-N accumulation was detected in any system, as the effluent concentration of $NO_2^-$-N never exceeded 0.05 mg.$L^{-1}$. During stage II, the start SND was comparable to stage I and the degree of SND reached 40% in SBR D and 59% in SBR E. No $NO_2^-$-N accumulation was observed as the average effluent concentration was 0.04 ± 0.02 mg $NO_2^-$-N.$L^{-1}$ and 0.03 ± 0.01 mg $NO_2^-$-N.$L^{-1}$, respectively for SBR D and SBR E. Literature reports a degree of SND up to 98% at low DO of 0.5 mg $O_2$.$L^{-1}$ and room temperature (Guo et al., 2013). In current study the degree of SND was incomplete, probably due to the relatively small granule size and the moderately high DO level during the aeration step (between 1.0 mg $O_2$.$L^{-1}$ and 2.0 mg $O_2$.$L^{-1}$).

### 3.2. AGS formation

#### 3.2.1. Feast/famine regime

The anaerobic DOC uptake and the related anaerobic P-release in both stages are presented in Figure 1. These results are linked to the above-mentioned $PO_4^{3-}$-P removal efficiency. A rapid increase of the anaerobic DOC uptake was observed in all systems during the first week of operation, indicating the fast adaptation of the microbial community to the applied anaerobic/aerobic operational strategy. During stage I, the reference reactor (SBR A) fed with VFAs, obtained the highest anaerobic P-release. In SBR B, an incomplete DOC uptake was observed (51.5 ± 10.6%) due to an insufficient uptake (10.1 ± 2.1%) of leucine (data according to *ex-situ* batch test). To the best of our knowledge, anaerobic uptake of leucine was never reported in literature before, but literature reports a low anaerobic P-release (maximum of 1.54 mg P.$gVSS^{-1}$) linked to the dosage of leucine (Nguyen et al., 2015). The reason for the lack of a sufficient anaerobic uptake and related P-release of leucine is still unclear and

must be examined in future research. An overall COD removal efficiency higher than 93% in SBR B indicates the consumption (cfr. oxidation) of leucine in the aerobic period rather than during the anaerobic phase. In SBR B, a low anaerobic P-release (maximum of 4.1 mg P.gVSS$^{-1}$) was observed, confirming the results of Qiu et al. (2019) who reported a moderate anaerobic P-release up to 7.33 mg P.gMLSS$^{-1}$ for glutamate and up to 7.37 mg P.gMLSS$^{-1}$ for aspartate. Nguyen et al. (2015) investigated twenty different amino acids in a conventional EBPR system, including glutamate and aspartate, with glycine yielding the highest P-release (up to 12.44 mg P.gVSS$^{-1}$). Values up to 3.10 mg P.gVSS$^{-1}$ and 6.81 mg P.gVSS$^{-1}$ respectively, were obtained when dosing glutamate and aspartate (Nguyen et al. 2015). Despite these findings, the anaerobic P-release in systems fed with amino acids was remarkably low in comparison to systems fed with VFAs as sole type of carbon source (Henriet et al., 2016; Wang et al., 2010; Weissbrodt et al., 2014). In SBR C, fed with glucose, a high anaerobic DOC uptake was observed, comparable to the reference reactor, but almost no anaerobic P-release was obtained. Oehmen et al. (2007) suggested that lower anaerobic P-release/DOC uptake ratios could indicate a possible GAO competition for the available substrate during the anaerobic step (Oehmen et al., 2007). More recent literature reported a dominance of GAOs over PAOs in EBPR systems fed with glucose (Layer et al., 2019; Wang et al., 2010). GAOs outcompete PAOs as they use glycogen as the energy source for the uptake of glucose. As a result, P-removal deteriorated. During stage II, the reference reactor (SBR D) and SBR E obtained comparable anaerobic DOC uptake and anaerobic P-release values. This observation confirms the outcome of Qiu et al. (2019), stating that VFAs were the most effective carbon sources for release and uptake of P.

### 3.2.2. Granulation

The operation of a granulation strategy (cfr. feast/famine regime) resulted in the improvement of the sludge characteristics. An evolution towards the densification of the sludge was observed in all reactor systems. Table 2 shows an overview of the parameters (SVI, ALE content and DV50) related to the morphology of the hybrid (granular and floccular) sludge. The SVI as well as the DV50 improved in all systems. During stage II, sludge morphology improvements were comparable in both systems. The availability of high fractions of easily degradable and diffusible organic substrates, such as VFAs, resulted in fast and excellent granulation (Adler & Holliger, 2020; Layer et al., 2019). Relative small granule sizes were obtained in the reference reactors (SBR A and SBR D). The differences in granulation between previously mentioned studies and current study is probably linked to the difference in reactor operation (higher COD gradient, feeding throughout the sludge bed, a short settling time (1 min)) and configuration (H/D ratio of 8.4). The results obtained in SBR B, SBR C and SBR E complement the study of Adler & Holliger (2020) who reported that wastewater containing complex monomeric compounds, e.g. amino acids and glucose, in addition to VFAs, has no negative impact on sludge characteristics and settling properties. The ALE content increased in all reactors. The presence of VFAs in SBR A, SBR D and SBR E resulted in a higher ALE content than in SBR B and SBR C. Recent literature reported the positive effect of VFAs on the ALE content of granular sludge (up to 261 ± 33 $mgVS_{ALE}.gVSS^{-1}$) (Schambeck et al., 2020).

### 3.2.3. *In-situ* $N_2O$ emissions

$N_2O$ emissions were calculated at the beginning and at the end of the study (Table 3). At the start of stage I the total $N_2O$-N emission was 0.48 ± 0.11% compared to the

329 total available nitrogen ($NH_4^+$-N) at the start of the aerobic phase of the SBR cycle.
330 These results are comparable to values reported in earlier studies about $N_2O$-N
331 emission monitoring in full-scale municipal (low-loaded EBPR) WWTPs (Foley et al.,
332 2010). At the end of the study, the $N_2O$-N emission was 1.62% in SBR A. In SBR B, no
333 $N_2O$ emission was detected. In SBR C, 1.14% of the total available nitrogen ($NH_4^+$-N)
334 was emitted as $N_2O$-N. The highest maximum $N_2O$ formation rate was detected in SBR
335 A. The reactor systems during stage II emitted 1.31 ± 0.16% $N_2O$-N at the start of the
336 experiment. At the end of stage II, SBR D and E emitted 6.25 and 3.53% $N_2O$-N
337 respectively. The results of stage II are comparable to a recent study of Jahn et al.
338 (2019). Moreover, both systems exhibited a significantly higher maximum $N_2O$
339 formation rate in comparison to the systems during stage I.

340 The combination of remnant $NH_4^+$ and high $NO_2^-$-N concentrations (cfr. nitritation
341 rather than full nitrification) is a strong trigger for $N_2O$ emissions (Rodriguez-Caballero
342 et al., 2013). In current study, only low concentrations of nitrite (maximum of 0.824 mg
343 $NO_2^-$-$N.L^{-1}$) could be detected in all systems. This observation excludes the impact of
344 the nitrification pathway on the overall $N_2O$ formation in these systems. Another main
345 factor stimulating formation of $N_2O$ is the PHA related denitrification (d-PAO)
346 metabolism. This slow PHA degradation process influences the activity of $N_2O$
347 reductase, leading to an accumulation of $N_2O$ (Kampschreur et al., 2009). The increase
348 in $N_2O$ emissions, except in SBR B (fed with amino acids), presumably indicates the
349 increasing importance of this metabolism over time on the formation of $N_2O$. In SBR B
350 an average anaerobic DOC uptake of 51.5 ± 10.6% was observed, leading to more COD
351 leakage into the aerobic phase and the corresponding availability of (easily) degradable

carbon for complete denitrification. Despite the relative low granule size in SBR B, this COD leakage consumes so much oxygen that the oxygen penetration depth decreases severely, which presumably explains the relative high SND efficiency (up to 44%) found in SBR B. Furthermore, $N_2O$ formation could be attributed to the low gene expression of the nosZ gene in *Accumulibacter* (Morales et al., 2010; Vieira et al., 2018). The enrichment of *Accumulibacter*, due to the presence of VFAs in the influent, probably led to the emission of $N_2O$ in SBR A, SBR D and SBR E. The application of different complex monomeric substrates (i.c. amino acids and glucose) in SBR B and SBR C, could lead to the enrichment of a significantly different microbial population, in which the nosZ gene was highly active. In the future, a gene expression study will be carried out to investigate the presence and activity of this gene.

### 3.3. *Ex-situ* batch experiments

#### 3.3.1. Nitrifying activity measurements

In both stages a similar progress of NOB/AOB activity ratio and qPCR quantification ratio was observed.The NOB/AOB activity ratio was (with exception of week 3 during stage II) always higher than 40% for all reactor systems indicating complete nitrification, without any suppression of NOB. The lack of NOB inhibition is probably the result of the moderately high DO level applied (between 1.0 and 2.0 mg $O_2.L^{-1}$) and the long aeration phase (at least 165 min) (Dobbeleers et al., 2017). Despite the complete nitrification in SBR A, SBR C, SBR D and SBR E, significant $N_2O$ emissions were observed in these reactors. This observation contrasts the results of Rodriguez-Caballero et al. (2013) that $N_2O$ emissions are minimised under full nitrification conditions (cfr. $N_2O$-N emission compared to the total available nitrogen ($NH_4^+$-N) of 1.22 ± 0.22% and 0.54 ± 0.07% under nitritation and full nitrification conditions

respectively). However, it supports the hypothesis of Vieira et al. (2018) that $N_2O$ formation is closely linked to the PHA related denitrification (d-PAO) metabolism and the inhibition of the nosZ gene in highly *Accumulibacter*-enriched systems. As already indicated, the COD leakage into the aerobic phase in SBR B presumably led to a complete denitrification using the leaked COD rather than the stimulation of a PHA related denitrification in that SBR.

### 3.3.2. Dosage of individual carbon substrates to adapted sludge

Batch tests were conducted to investigate the individual effects of the different carbon substrates on the EBPR activity (Figure 2). For SBR A, both acetate and propionate resulted in an almost complete anaerobic DOC uptake and a comparable anaerobic P-release. With sludge from SBR B, the dosage of leucine resulted in no anaerobic DOC uptake which explains the incomplete anaerobic DOC uptake observed in the overall follow-up during the *in-situ* cycle measurements (Figure 1). According to Qiu et al. (2019), dosage of glutamate and aspartate results in lower anaerobic P:C ratios (0.16-0.43 mol P.mol $C^{-1}$ and 0.17-0.48 mol P.mol $C^{-1}$ respectively for glutamate and aspartate) in comparison to VFAs (anaerobic P:C ratio of 0.35-0.66 mol P. mol $C^{-1}$ for acetate). The dosage of glucose resulted in a high anaerobic DOC uptake but no anaerobic P-release confirming the results of the *in-situ* tests. This pattern was also reported by other researchers, evidencing that glycogen can replace/complement poly-P to provide energy in systems fed with glucose (Wang et al., 2010). During stage II, leucine was no longer added as carbon substrate. Dosage of acetate and propionate to biomass of SBR D and SBR E yielded similar results as those with sludge from SBR A. In comparison with the other carbon sources applied in SBR E, VFAs yielded much

399 higher anaerobic P-release values. These findings confirm the hypothesis of Qiu et al.
400 (2019) that VFAs are the most effective carbon sources for release and uptake of P. In
401 comparison to SBR B, dosage of glutamate and aspartate to sludge of SBR E resulted in
402 a higher anaerobic DOC uptake but a lower anaerobic P-release. A possible explanation
403 could be the higher abundance of fermentative organisms in SBR E, resulting in an
404 improvement of the fermentation capacity. In comparison with direct uptake of amino
405 acids, fermentation generates energy which reduces the amount of poly-P that has to
406 be hydrolysed to take up the substrate, resulting in a lower anaerobic P-release
407 (Marques et al., 2017). With sludge from SBR C and SBR E, the dosage of glucose,
408 resulted in an almost complete anaerobic DOC uptake and no anaerobic P-release.
409 Both results are similar and confirm that glucose did not support any EBPR activity.

410 **3.3.3. Dosage of individual carbon substrates to non-adapted sludge**

411 In a second series of batch experiments individual substrates were dosed to sludge
412 from reactors that did not receive these substrates during long term reactor operation
413 (Figure 3). The dosage of other substrates than VFAs to sludge from SBR A resulted in
414 an anaerobic DOC uptake higher than 80% but low anaerobic P-release values.
415 Interestingly, the dosage of glucose to sludge from SBR B (fed with amino acids)
416 resulted in a significantly higher anaerobic P-release than any other sludge receiving
417 glucose. An explanation could be the higher abundance of fermentative organisms in
418 SBR B in comparison to SBR A, producing VFAs from glucose. In case of sludge from
419 SBR C, high anaerobic DOC uptake was observed for all carbon sources applied, but no
420 anaerobic P-release, even with VFAs. These results are in contrast to all the other
421 experiments, indicating that the operation of SBR C, fed with glucose only, resulted in

422 the enrichment of GAOs rather than PAOs. The low anaerobic P-release observed in
423 batch tests with sludge from SBR D (a stable EBPR system) confirm that glucose leads
424 to the lowest PAO activity, in comparison to the other carbon sources applied. Glucose
425 could serve as a substrate for EBPR indirectly through acetate, propionate or lactate
426 utilisation by PAOs. This would require the co-existence of fermentative bacteria
427 producing previously mentioned metabolites from glucose. However, as stated by
428 Zengin et al. (2010), continuous glucose feeding probably resulted in the disruption of
429 EBPR in favour of direct utilisation of glucose by GAOs and abundance of GAOs over
430 PAOs.

431 **3.4. Microbial management**

432 **3.4.1. Effects of the applied carbon source on the competition between**
433 ***Accumulibacter* and *Competibacter***

434 Figure 4 shows the amount of target cells per g biomass for *Accumulibacter* and
435 *Competibacter*. *Accumulibacter* was enriched in alle reactors, except in SBR C (fed with
436 glucose). This confirms the results of both *in*- and *ex-situ* experiments in which EPBR
437 activity in all these systems was detected. Interestingly, the enrichment of
438 *Accumulibacte*r in those systems was significantly higher than *Competibacter*.
439 Literature reports that the occurrence of GAO populations may be controlled by the
440 presence of carbon in excess of what is required for P removal (Nielsen et al., 2019).
441 The study of Nielsen et al. (2019) claims that a moderate amount of GAOs may be a
442 good sign for efficient EPBR because they indicate a surplus of organics. Despite the
443 fact that literature reports that the use of glucose stimulates GAOs rather than PAOs,
444 almost no enrichment of *Competibacter* was found in SBR C (Layer et al., 2019; Zengin
445 et al., 2010). This observation suggests that other GAOs than *Competibacter* were

446 enriched and confirm that *Competibacter* is not able to use glucose as carbon source
447 (Nierychlo et al., 2020). In stage II, a comparable enrichment of *Accumulibacter* was
448 found in both SBRs. This indicates that the presence of VFAs in the influent of SBR E
449 resulted in the enrichment of PAOs (in comparison to SBR B and SBR C). The
450 importance of VFAs in the influent regarding the PAO-GAO interactions and the
451 achievement of a stable EPBR activity is thereby emphasized again. These findings
452 confirm that *Accumulibacter* provides a robustness to biological dephosphatation as
453 this organism was highly enriched in SBR A, SBR D and SBR E.

454 ### 3.4.2. Importance of VFAs to the overall microbial community

455 Microbial analysis through 16S rRNA gene amplicon sequencing was performed to
456 gain insights into the effect of the applied carbon sources on the microbial
457 enrichments. NMDS analysis using taxonomic (Bray-Curtis) metrics confirms the
458 differences in microbial community composition between the seed sludge and the
459 other reactor systems (Figure 5a). Permutational multivariate analysis of variance
460 (ADONIS) was used to determine if bacterial community composition between all
461 reactor systems was statistically different ($P=0.001 < 0.05$). Assumption of
462 homogeneity of multivariate dispersion was taken into account using ANOVA ($P = 0.511 > 0.05$). Figure 5b shows a PCA plot of the microbial community structure at
464 genus level with sample distribution patterns during the operation of all reactor
465 systems. Progressive changes in the microbial communities are visualised. The PCA
466 plot shows that the inoculum of all systems was similar. Furthermore, the origin of this
467 plot indicates a core population which is stably present in all microbial samples during
468 the entire operation. While the process conditions (e.g. OLR, pH, temperature,

feast/famine regime) remained unchanged throughout the entire experiment in all reactor systems, the PCA plot clearly illustrates the similar microbial enrichment pattern in reactor systems in which VFAs were present in the influent (SBR A, SBR D and SBR E). However, the evolution of SBR D and SBR E is more limited as the operational time was shorter. As already indicated, VFAs stimulate the enrichment of *Accumulibacter*, while other complex substances lead to substrate/species-specific enrichments (Adler & Holliger, 2020; Layer et al., 2019). This study confirms that the presence of VFAs is decisive in the enrichment of the microbial population and the stability of EBPR (Qiu et al., 2019). The evolution of SBR B is significantly different from the other reactors, indicating the low presence of PAOs, absence of GAOs and the distinct enrichment of *Burkholderiaceae* organisms. This family, belonging to the order of *Burkholderiales*, is phenotypically, metabolically and ecologically extremely diverse and includes both strict aerobic and facultatively anaerobic chemoorganotrophs, as well as obligate and facultative chemolithotrophs. They are able to produce PHB and related homopolyesters and/or copolymers and accumulate them intracellularly directly out of amino acids (Coenye, 2014). The anaerobic storage of carbon, without the fermentation towards VFAs will lead to a negative effect on the presence of non-fermentative PAOs (e.g. *Accumulibacter*) (Nielsen et al., 2019). Hence, the low abundance of PAOs in SBR B is linked to the high abundance of non-fermentative organisms and vice-versa. A recent study, focussing on functional gene analysis, suggests members of the *Burkholderiaceae* family as possible candidates for the reduction of $N_2O$ to $N_2$ (Hetz & Horn, 2021). The enrichment of some members of this family in SBR B probably led to the significant lack of $N_2O$ emission during SND.

492 *Tetraspheara*, a putative fermentative PAO was not enriched in SBR B, although this
493 organism is associated with the anaerobic uptake of amino acids and the storage as
494 glycogen and/or fermentation to acetate (Marques et al., 2017; Nielsen et al., 2019).
495 As indicated by Nielsen et al. (2019), this could be partly due to an extraction bias as
496 this genus is underestimated by standard DNA extraction procedures. The moderate
497 anaerobic P-release found during the entire operation of SBR B indicates that this
498 underestimation of *Tetraspheara* is rather unlikely. Furthermore, no GAOs were found
499 during the entire operation of SBR B. The enrichment of GAOs and
500 *Saccharimonadaceae*, resulted in a slightly different trajectory of the microbial
501 progression in SBR C. Results of SBR C confirm the outcome of Layer et al. (2019). They
502 indicate the enrichment of putative GAOs (*Propionivibrio* and *Micropruina)* rather than
503 *Competibacter* when using glucose as sole carbon source. *Propionivibrio* and
504 *Micropruina* are definied as fermentative GAO (fGAOs) as they use the energy and
505 carbon from fermentation for growth and the storage of glycogen (Nielsen et al.,
506 2019). Another recent study states that the current models of the competition
507 between fermentative PAOs (fPAOs)/fGAOs and non-fermentative PAOs/GAOs are too
508 simplistic and that the amount of (potential) carbon storage by these fPAOs and fGAOs
509 could be underestimated (McIlroy et al., 2018). This hypothesis is highly plausible as,
510 according to the low availability of VFAs, this presumably explains the low abundance
511 of *Accumulibacter* as well *as Competibacter* in SBR C. The study of Nielsen et al. (2019)
512 confirms the denitrifying capacity of *Competibacter* and indicates a rather unknown
513 genomic potential of *Propionivibrio* and *Micropruina* for nitrate and nitrite reduction.
514 The low SND found in SBR C is most likely correlated to the lack of *Competibacter* in

515 the microbial community profile as well as the incompetence of *Propionivibrio* and
516 *Micropruina* to denitrify. Furthermore, glucose-fermenting organisms were enriched in
517 SBR C. These organisms belong to the same family, namely *Saccharimonadaceae*, and
518 were not found in SBR A and SBR B. So far, little is known about the phylogeny and
519 physiology of these organisms, resulting in an insufficient knowledge whether these
520 organisms are characterised by an obligate fermentative metabolism (cfr. taking up
521 glucose and releasing acetate and/or lactacte) or store it as PHA and subsequently
522 consume it during the aerobic period of the applied feast/famine regime (Adler &
523 Holliger, 2020). Attenuated total reflection Fourier transform infrared (ATR-FTIR)
524 spectroscopy is proposed in literature as a method for rapid (online) quantification of
525 PHA (Arcos-Hernandez et al., 2010; Isak et al., 2016). Application of this technique
526 could reduce the speculative outcome and improve the knowledge associated with
527 PHA related polymers in mixed culture approaches. Results from SBR D and SBR E
528 confirm the development of a stable EBPR system due to a sufficient enrichment of
529 PAOs rather than GAOs. The presence of VFAs in the influent of those systems and the
530 related enrichment of *Accumulibacter* confirm the important role of this organism in
531 the achievement of a stable EBPR system. Although amino acids and glucose were
532 present (next to VFAs) in the influent of SBR E, substrate-specific enrichment of
533 organisms belonging to the *Burkholderiaceae* family or *Saccharimonadaceae* was not
534 observed.

535 **4. Conclusion**

536 The impact of fermentable compounds on the formation of AGS-EBPR was
537 investigated. Anaerobic DOC uptake and sludge densification were observed in all

systems. During future investigation, qualification of intracellular PHA using ATR-FTIR could lead to improved insights in the carbon uptake/consumption applying different substrates. Stable EBPR, related to *Accumulibacter*, was only obtained when VFAs were present as sole substrate or in a mixture. The presence of *Accumulibacter* clearly correlated with the formation of $N_2O$. Future research should examine the expression of key genes involved in the denitrification pathway in response to the application of various fermentable compounds.

## 5. Supplementary Material

E-supplementary data for this work can be found in e-version of this paper online.

**Table S1.** Summary of wastewater characteristics: carbon source (COD), $NH_4^+$-N and $PO_4^{3-}$-P in different reactors.

**Table S2.** Target, cell copy number, primers and qPCR conditions used during molecular quantification.

**Figure S1.** NOB/AOB activity ratio (%) and NOB/AOB absolute quantification ratio (%) throughout the entire operational period of all reactor systems during stage I (a) and stage II (b).

## 6. Data Availability

The datasets generated and/or analysed during the current study are available from the corresponding author on reasonable request.

## 7. Acknowledgements

This research was supported by the University of Antwerp (University Research Fund (BOF)), supporting fundamental research (grant number FFB190191), carried out at the BioWAVE research group, part of the faculty of Applied Engineering.

## 8. References

1. Adler, A., Holliger, C. 2020. Multistability and Reversibility of Aerobic Granular Sludge Microbial Communities Upon Changes From Simple to Complex Synthetic Wastewater and Back. *Frontiers in microbiology*, **11**, 574361-574361.
2. American Public Health Association (APHA). 2012. Standard Methods for the Examination of Water and Wastewater, 22nd Edition. New York.
3. Andersen, K.S., Kirkegaard, R.H., Karst, S.M., Albertsen, M. 2018. ampvis2: an R package to analyse and visualise 16S rRNA amplicon data. *bioRxiv*, 299537.

4. Arcos-Hernandez, M.V., Gurieff, N., Pratt, S., Magnusson, P., Werker, A., Vargas, A., Lant, P. 2010. Rapid quantification of intracellular PHA using infrared spectroscopy: An application in mixed cultures. *Journal of Biotechnology*, **150**(3), 372-379.
5. Caluwe, M., Dobbeleers, T., D'Aes, J., Miele, S., Akkermans, V., Daens, D., Geuens, L., Kiekens, F., Blust, R., Dries, J. 2017. Formation of aerobic granular sludge during the treatment of petrochemical wastewater. *Bioresour Technol*, **238**, 559-567.
6. Carvalho, G., Lemos, P.C., Oehmen, A., Reis, M.A.M. 2007. Denitrifying phosphorus removal: Linking the process performance with the microbial community structure. *Water Research*, **41**(19), 4383-4396.
7. Coenye, T. 2014. The Family Burkholderiaceae. in: *The Prokaryotes: Alphaproteobacteria and Betaproteobacteria*, (Eds.) E. Rosenberg, E.F. DeLong, S. Lory, E. Stackebrandt, F. Thompson, Springer Berlin Heidelberg. Berlin, Heidelberg, pp. 759-776.
8. de Kreuk, M.K., Kishida, N., Tsuneda, S., van Loosdrecht, M.C.M. 2010. Behavior of polymeric substrates in an aerobic granular sludge system. *Water Research*, **44**(20), 5929-5938.
9. de Kreuk, M.K., van Loosdrecht, M.C. 2004. Selection of slow growing organisms as a means for improving aerobic granular sludge stability. *Water Sci Technol*, **49**(11-12), 9-17.
10. Dobbeleers, T., Caluwé, M., Dockx, L., Daens, D., D'aes, J., Dries, J. 2020. Biological nutrient removal from slaughterhouse wastewater via nitritation/denitritation using granular sludge: an onsite pilot demonstration. *Journal of Chemical Technology & Biotechnology*, **95**(1), 111-122.
11. Dobbeleers, T., Daens, D., Miele, S., D'aes, J., Caluwé, M., Geuens, L., Dries, J. 2017. Performance of aerobic nitrite granules treating an anaerobic pre-treated wastewater originating from the potato industry. *Bioresource Technology*, **226**, 211-219.
12. EPA. 2017. Understanding Global Warming Potential, United States Environmental Protection Agency.
13. Felz, S., Vermeulen, P., van Loosdrecht, M.C.M., Lin, Y.M. 2019. Chemical characterization methods for the analysis of structural extracellular polymeric substances (EPS). *Water Research*, **157**, 201-208.
14. Foley, J., de Haas, D., Yuan, Z., Lant, P. 2010. Nitrous oxide generation in full-scale biological nutrient removal wastewater treatment plants. *Water Res*, **44**(3), 831-44.
15. Guo, J., Zhang, L., Chen, W., Ma, F., Liu, H., Tian, Y. 2013. The regulation and control strategies of a sequencing batch reactor for simultaneous nitrification and denitrification at different temperatures. *Bioresour Technol*, **133**, 59-67.
16. Henriet, O., Meunier, C., Henry, P., Mahillon, J. 2016. Improving phosphorus removal in aerobic granular sludge processes through selective microbial management. *Bioresour Technol*, **211**, 298-306.
17. Hetz, S.A., Horn, M.A. 2021. Burkholderiaceae Are Key Acetate Assimilators During Complete Denitrification in Acidic Cryoturbated Peat Circles of the Arctic Tundra. *Frontiers in Microbiology*, **12**(151).
18. Isak, I., Patel, M., Riddell, M., West, M., Bowers, T., Wijeyekoon, S., Lloyd, J. 2016. Quantification of polyhydroxyalkanoates in mixed and pure cultures biomass by Fourier transform infrared spectroscopy: comparison of different approaches. *Lett Appl Microbiol*, **63**(2), 139-46.
19. Jahn, L., Svardal, K., Krampe, J. 2019. Nitrous oxide emissions from aerobic granular sludge. *Water Science and Technology*, **80**(7), 1304-1314.
20. Kampschreur, M.J., Temmink, H., Kleerebezem, R., Jetten, M.S., van Loosdrecht, M.C. 2009. Nitrous oxide emission during wastewater treatment. *Water Res*, **43**(17), 4093-103.

21. Kozich, J.J., Westcott, S.L., Baxter, N.T., Highlander, S.K., Schloss, P.D. 2013. Development of a dual-index sequencing strategy and curation pipeline for analyzing amplicon sequence data on the MiSeq Illumina sequencing platform. *Appl Environ Microbiol*, **79**(17), 5112-20.
22. Layer, M., Adler, A., Reynaert, E., Hernandez, A., Pagni, M., Morgenroth, E., Holliger, C., Derlon, N. 2019. Organic substrate diffusibility governs microbial community composition, nutrient removal performance and kinetics of granulation of aerobic granular sludge. *Water Research X*, **4**, 100033.
23. Marques, R., Santos, J., Nguyen, H., Carvalho, G., Noronha, J.P., Nielsen, P.H., Reis, M.A.M., Oehmen, A. 2017. Metabolism and ecological niche of Tetrasphaera and Ca. Accumulibacter in enhanced biological phosphorus removal. *Water Res*, **122**, 159-171.
24. McIlroy, S.J., Onetto, C.A., McIlroy, B., Herbst, F.-A., Dueholm, M.S., Kirkegaard, R.H., Fernando, E., Karst, S.M., Nierychlo, M., Kristensen, J.M., Eales, K.L., Grbin, P.R., Wimmer, R., Nielsen, P.H. 2018. Genomic and in Situ Analyses Reveal the Micropruina spp. as Abundant Fermentative Glycogen Accumulating Organisms in Enhanced Biological Phosphorus Removal Systems. *Frontiers in Microbiology*, **9**(1004).
25. Morales, S.E., Cosart, T., Holben, W.E. 2010. Bacterial gene abundances as indicators of greenhouse gas emission in soils. *Isme j*, **4**(6), 799-808.
26. Nguyen, H.T.T., Kristiansen, R., Vestergaard, M., Wimmer, R., Nielsen, P.H. 2015. Intracellular Accumulation of Glycine in Polyphosphate-Accumulating Organisms in Activated Sludge, a Novel Storage Mechanism under Dynamic Anaerobic-Aerobic Conditions. *Applied and environmental microbiology*, **81**(14), 4809-4818.
27. Nielsen, P.H., McIlroy, S.J., Albertsen, M., Nierychlo, M. 2019. Re-evaluating the microbiology of the enhanced biological phosphorus removal process. *Current Opinion in Biotechnology*, **57**, 111-118.
28. Nielsen, P.H., Saunders, A.M., Hansen, A.A., Larsen, P., Nielsen, J.L. 2012. Microbial communities involved in enhanced biological phosphorus removal from wastewater--a model system in environmental biotechnology. *Curr Opin Biotechnol*, **23**(3), 452-9.
29. Nierychlo, M., Andersen, K.S., Xu, Y., Green, N., Jiang, C., Albertsen, M., Dueholm, M.S., Nielsen, P.H. 2020. MiDAS 3: An ecosystem-specific reference database, taxonomy and knowledge platform for activated sludge and anaerobic digesters reveals species-level microbiome composition of activated sludge. *Water Research*, **182**, 115955.
30. Oehmen, A., Carvalho, G., Lopez-Vazquez, C., van Loosdrecht, M., Reis, M. 2010. Incorporating microbial ecology into the metabolic modelling of polyphosphate accumulating organisms and glycogen accumulating organisms. *Water research*, **44**, 4992-5004.
31. Oehmen, A., Lemos, P.C., Carvalho, G., Yuan, Z., Keller, J., Blackall, L.L., Reis, M.A.M. 2007. Advances in enhanced biological phosphorus removal: From micro to macro scale. *Water Research*, **41**(11), 2271-2300.
32. Oksanen, J., Blanchet, F.G., Kindt, R., Legendre, P., Minchin, P., O'Hara, B., Simpson, G., Solymos, P., Stevens, H., Wagner, H. 2015. Vegan: Community Ecology Package. *R Package Version 2.2-1*, **2**, 1-2.
33. Pronk, M., de Kreuk, M.K., de Bruin, B., Kamminga, P., Kleerebezem, R., van Loosdrecht, M.C. 2015. Full scale performance of the aerobic granular sludge process for sewage treatment. *Water Res*, **84**, 207-17.
34. Qiu, G., Zuniga-Montanez, R., Law, Y., Thi, S.S., Nguyen, T.Q.N., Eganathan, K., Liu, X., Nielsen, P.H., Williams, R.B.H., Wuertz, S. 2019. Polyphosphate-accumulating organisms in full-scale tropical wastewater treatment plants use diverse carbon sources. *Water Research*, **149**, 496-510.

35. Rodriguez-Caballero, A., Ribera, A., Balcázar, J.L., Pijuan, M. 2013. Nitritation versus full nitrification of ammonium-rich wastewater: comparison in terms of nitrous and nitric oxides emissions. *Bioresour Technol*, **139**, 195-202.

36. Rubio-Rincón, F.J., Lopez-Vazquez, C.M., Welles, L., van Loosdrecht, M.C.M., Brdjanovic, D. 2017. Cooperation between Candidatus Competibacter and Candidatus Accumulibacter clade I, in denitrification and phosphate removal processes. *Water Res*, **120**, 156-164.

37. Schambeck, C.M., Girbal-Neuhauser, E., Böni, L., Fischer, P., Bessière, Y., Paul, E., da Costa, R.H.R., Derlon, N. 2020. Chemical and physical properties of alginate-like exopolymers of aerobic granules and flocs produced from different wastewaters. *Bioresource Technology*, **312**, 123632.

38. Stes, H., Aerts, S., Caluwé, M., Dobbeleers, T., Wuyts, S., Kiekens, F., D'Aes, J., De Langhe, P., Dries, J. 2018. Formation of aerobic granular sludge and the influence of the pH on sludge characteristics in a SBR fed with brewery/bottling plant wastewater. *Water Sci Technol*, **77**(9-10), 2253-2264.

39. Stokholm-Bjerregaard, M., McIlroy, S.J., Nierychlo, M., Karst, S.M., Albertsen, M., Nielsen, P.H. 2017. A Critical Assessment of the Microorganisms Proposed to be Important to Enhanced Biological Phosphorus Removal in Full-Scale Wastewater Treatment Systems. *Front Microbiol*, **8**, 718.

40. van den Berg, L., Kirkland, C.M., Seymour, J.D., Codd, S.L., van Loosdrecht, M.C.M., de Kreuk, M.K. 2020. Heterogeneous diffusion in aerobic granular sludge. *Biotechnology and Bioengineering*, **117**(12), 3809-3819.

41. Vieira, A., Ribera-Guardia, A., Marques, R., Barreto Crespo, M.T., Oehmen, A., Carvalho, G. 2018. The link between the microbial ecology, gene expression, and biokinetics of denitrifying polyphosphate-accumulating systems under different electron acceptor combinations. *Appl Microbiol Biotechnol*, **102**(15), 6725-6737.

42. Vishniac, W., Santer, M. 1957. The thiobacilli. *Bacteriological reviews*, **21**(3), 195-213.

43. Wagner, J., Guimarães, L.B., Akaboci, T.R.V., Costa, R.H.R. 2015a. Aerobic granular sludge technology and nitrogen removal for domestic wastewater treatment. *Water Science and Technology*, **71**(7), 1040-1046.

44. Wagner, J., Weissbrodt, D.G., Manguin, V., Ribeiro da Costa, R.H., Morgenroth, E., Derlon, N. 2015b. Effect of particulate organic substrate on aerobic granulation and operating conditions of sequencing batch reactors. *Water Research*, **85**, 158-166.

45. Wang, Q., Yao, R., Yuan, Q., Gong, H., Xu, H., Ali, N., Jin, Z., Zuo, J., Wang, K. 2018. Aerobic granules cultivated with simultaneous feeding/draw mode and low-strength wastewater: Performance and bacterial community analysis. *Bioresource Technology*, **261**, 232-239.

46. Wang, Y., Jiang, F., Zhang, Z., Xing, M., Lu, Z., Wu, M., Yang, J., Peng, Y. 2010. The long-term effect of carbon source on the competition between polyphosphorus accumulating organisms and glycogen accumulating organism in a continuous plug-flow anaerobic/aerobic (A/O) process. *Bioresource Technology*, **101**(1), 98-104.

47. Weissbrodt, D.G., Shani, N., Holliger, C. 2014. Linking bacterial population dynamics and nutrient removal in the granular sludge biofilm ecosystem engineered for wastewater treatment. *FEMS Microbiol Ecol*, **88**(3), 579-95.

48. Zengin, G.E., Artan, N., Orhon, D., Chua, A.S., Satoh, H., Mino, T. 2010. Population dynamics in a sequencing batch reactor fed with glucose and operated for enhanced biological phosphorus removal. *Bioresour Technol*, **101**(11), 4000-5.

49. Zengin, G.E., Artan, N., Orhon, D., Satoh, H., Mino, T. 2011. Effect of aspartate and glutamate on the fate of enhanced biological phosphorus removal process and microbial community structure. *Bioresour Technol*, **102**(2), 894-903.

## 9. Tables and Figures

**Table 1.** Summary of effluent $PO_4^{3-}$-P concentration ($mg.L^{-1}$), total P-removal efficiency (%), $NO_3^-$-N ($mg.L^{-1}$) concentration and total N-removal efficiency (%) for the different reactors.

| | | Effluent $PO_4^{3-}$-P ($mg.L^{-1}$) | | | P-removal (%) | | | Effluent $NO_3^-$-N ($mg.L^{-1}$) | | | N-removal (%) | | |
|---|---|---|---|---|---|---|---|---|---|---|---|---|---|
| **SBR** | **Carbon source (COD)** | **Min** | **Max** | **Average ± SD** | **Min** | **Max** | **Average ± SD** | **Min** | **Max** | **Average ± SD** | **Min** | **Max** | **Average ± SD** |
| **A** | VFAs | 0.0 | 1.4 | 0.3 ± 0.4 | 96.9 | 100.0 | 99.3 ± 0.9 | 9.9 | 14.2 | 11.8 ± 1.6 | 24.6 | 67.6 | 42.6 ± 12.4 |
| **B** | Amino acids | 0.0 | 29.0 | 8.7 ± 8.9 | 35.6 | 100.0 | 80.6 ± 19.7 | 8.4 | 13.4 | 10.2 ± 1.2 | 30.5 | 60.3 | 40.8 ± 7.8 |
| **C** | Glucose | 4.0 | 19.8 | 11.3 ± 4.7 | 17.8 | 91.1 | 67.8 ± 20.0 | 10.4 | 14.4 | 12.4 ± 1.4 | 22.3 | 64.3 | 38.0 ± 11.5 |
| **D** | VFAs | 0.0 | 1.2 | 0.6 ± 0.4 | 97.3 | 100.0 | 98.6 ± 1.0 | 3.9 | 5.8 | 4.8 ± 0.8 | 54.0 | 86.7 | 73.0 ± 9.9 |
| **E** | Mix | 0.0 | 1.6 | 0.6 ± 0.5 | 96.4 | 100.0 | 98.7 ± 1.2 | 2.9 | 5.2 | 3.4 ± 0.9 | 62.6 | 88.6 | 75.3 ± 8.4 |

677 **Table 2.** Summary of the parameters (SVI (n=5), ALE (n=1) and DV50 (n=2)) at the start and the end (last 14 days) of operation.

| **SBR** | **Start** | | | | **End of operation** | | | |
|---|---|---|---|---|---|---|---|---|
| | SVI ($mL.gMLSS^{-1}$) | $SVI_5/SVI_{30}$ | ALE content ($mgVS_{ALE}.gVSS^{-1}$) | DV50 (µm) | SVI ($mL.gMLSS^{-1}$) | $SVI_5/SVI_{30}$ | ALE content ($mgVS_{ALE}.gVSS^{-1}$) | DV50 (µm) |
| **A** | | | | | 52.1 ± 3.0 | 1.47 ± 0.04 | 405 | 170.5 ± 6.4 |
| **B** | 73.3 | 2.14 | 112 | 141 | 59.3 ± 4.4 | 1.83 ± 0.09 | 207 | 144.0 ± 11.3 |
| **C** | | | | | 40.7 ± 1.1 | 1.80 ± 0.03 | 284 | 211.5 ± 13.4 |
| **D** | 62.2 | 2.30 | 195 | 118 | 37.6 ± 1.8 | 1.95 ± 0.05 | 345 | 209.0 ± 19.1 |
| **E** | | | | | 38.4 ± 3.5 | 1.63 ± 0.06 | 337 | 235.3 ± 25.6 |

678

679 **Table 3.** Overview of the total $N_2O$-N emission (%$N_2O$) relative to the total available nitrogen ($NH_4^+$-N) at the start of the aerobic
680 phase of the SBR cycle and the maximum $N_2O$ formation rate (µg $N_2O$-N.(gVSS.L.h)$^{-1}$) at the first and the last week of the reactor
681 system.

| SBR | Start | | End of operation | |
|---|---|---|---|---|
| | % $N_2O$ | Maximum $N_2O$ formation rate (µg $N_2O$-N.(gVSS.L.h)$^{-1}$) | % $N_2O$ | Maximum $N_2O$ formation rate (µg $N_2O$-N.(gVSS.L.h)$^{-1}$) |
| **A** | 0.61 | 3.12 | 1.62 | 6.02 |
| **B** | 0.39 | 1.24 | 0.00 | 0.00 |
| **C** | 0.45 | 1.88 | 1.14 | 2.52 |
| **D** | 1.42 | 4.77 | 6.25 | 20.30 |
| **E** | 1.20 | 2.09 | 3.53 | 11.95 |

682

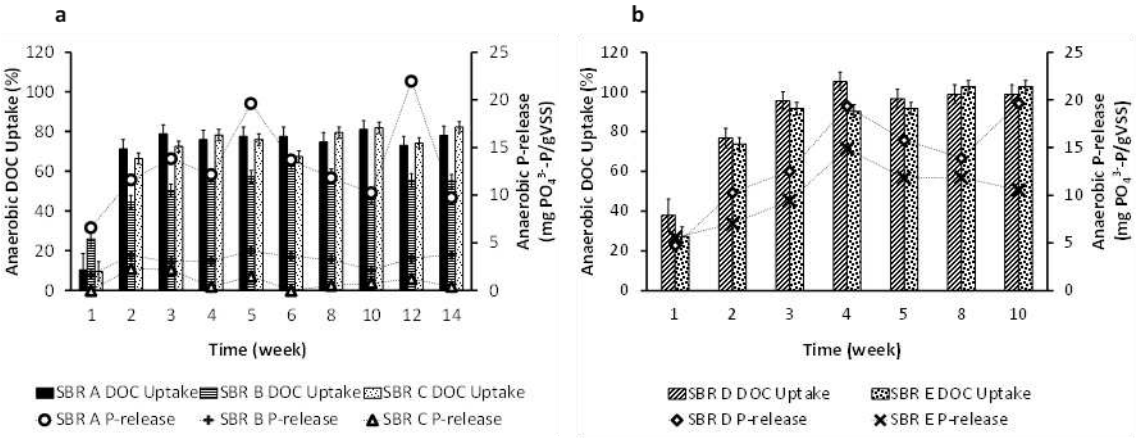


683

684 **Figure 1.** In-situ cycle measurements of DOC uptake (%) and P-release (mg $PO_4^{3-}$-P/gVSS) during the entire anaerobic phase during

685 stage I (a) and stage II (b).

686

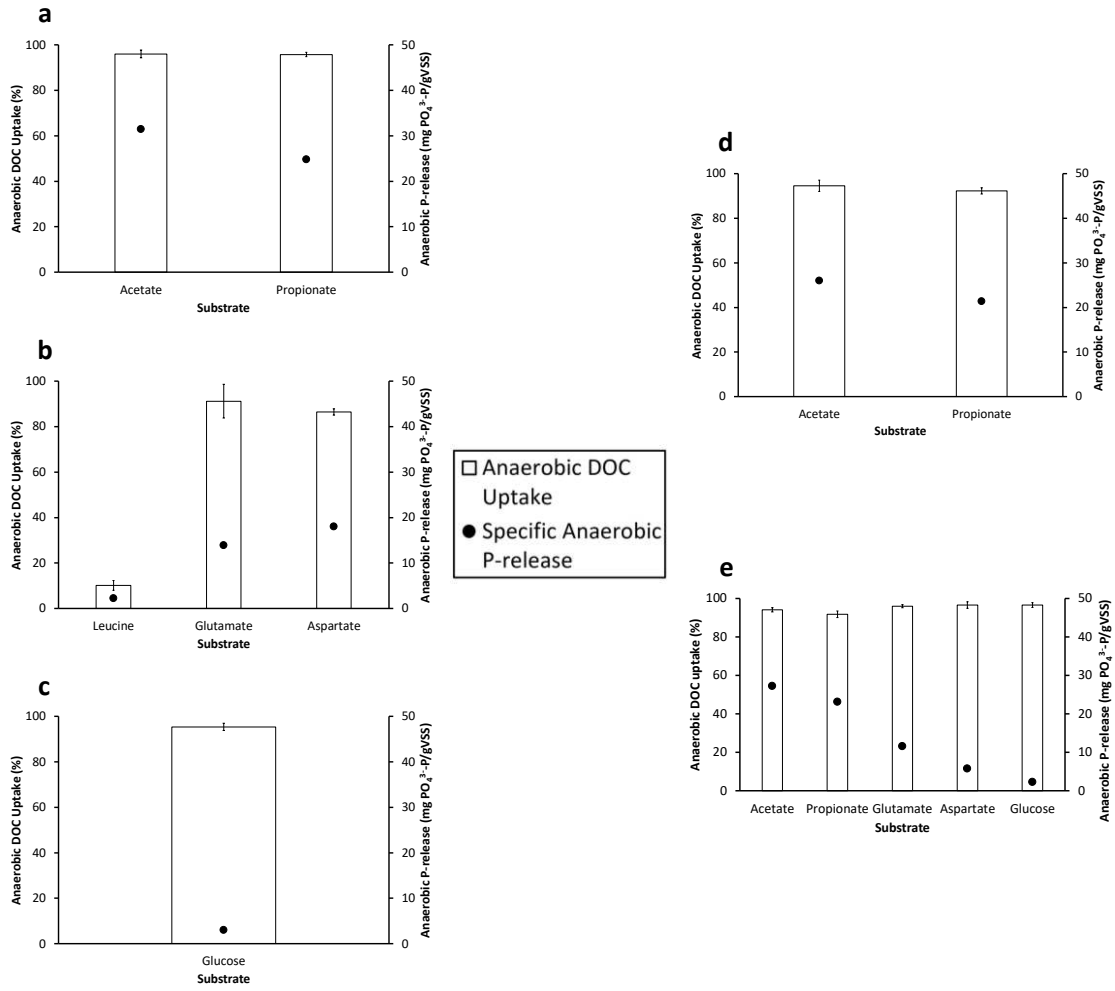


687

688 **Figure 2.** DOC uptake (%) and P-release (mg $PO_4^{3-}$-P.gVSS$^{-1}$) in *ex-situ* batch experiments with sludge taken from the different

689 reactors at the end of stage I and stage II. Individual substrates were dosed to sludge from SBR A (a), SBR B (b), SBR C (c), SBR D (d)

690 and SBR E (e).

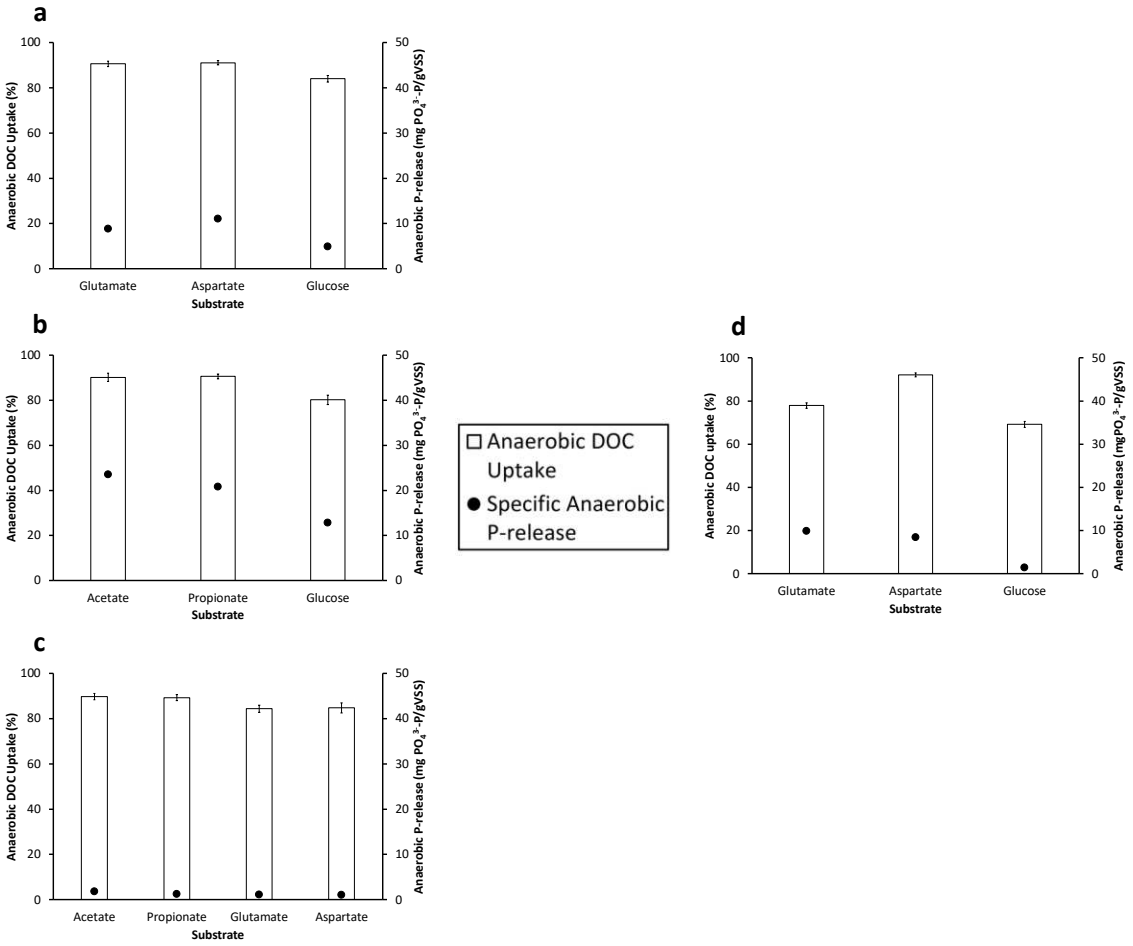


**Figure 3.** DOC uptake (%) and P-release (mg $PO_4^{3-}$-P.$gVSS^{-1}$) in *ex*-situ batch experiments with sludge taken from the different reactors at the end of stage I and stage II. Individual substrates were dosed to sludge from SBR A (a), SBR B (b), SBR C (c) and SBR D (d), that did not receive these substrates during the regular reactor operation.

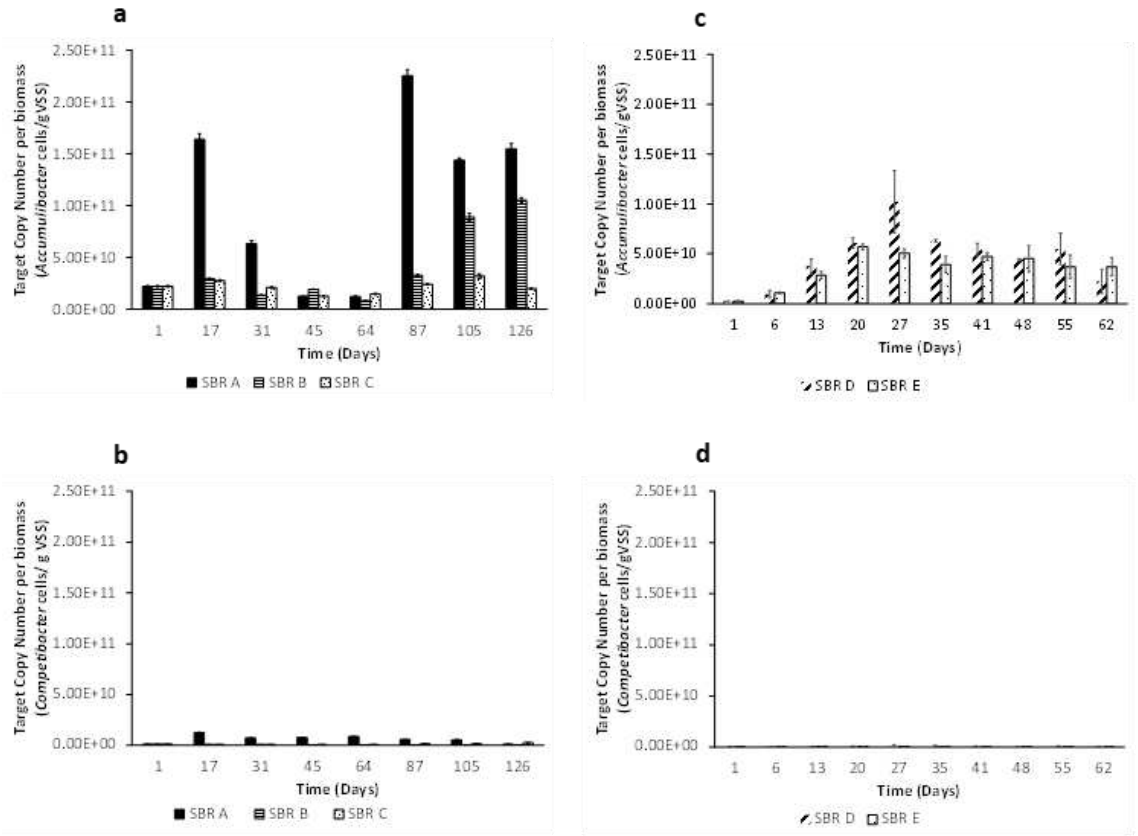


695

696 **Figure 4.** Evolution of *Accumulibacter* and *Competibacter* target cells per g biomass (cells/gVSS) during stage I (a-b) and stage II (c-
697 d).

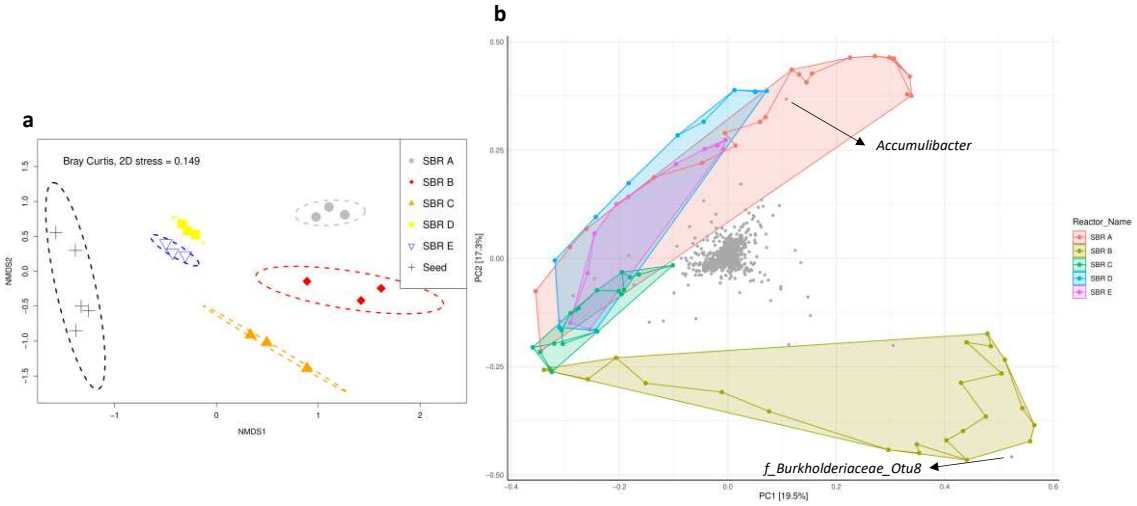


**Figure 5.** Nonmetric multidimensional scaling (NMDS) plot (OTU-based) of all reactor systems based on Bray-Curtis. The ellipse indicates that a random assemblage of the corresponding samples (in triplicate) falls in within a confidence of 0.95 (a). Samples, included in this analysis, correspond to end of the operational period of each reactor system. Principal component analysis (PCA) plot of the microbial community structure at genus level using the MiDAS 3.7 database with sample (triplicate) distribution patterns during the operation of all reactor systems (b). Each grey dot represents an unique read found in the microbial community (cfr. similarity threshold of 97%). PC1 and PC2 values include a relatively wide variability found within the different microbial communities.